On the theory of the Mott transition in the paramagnetic phase

1991 J. Phys.: Condens. Matter 3 1475

(http://iopscience.iop.org/0953-8984/3/11/009)

J. Phys.: Condens. Matter 3 (1991) 1475–1491. Printed in the UK

On the theory of the Mott transition in the paramagnetic phase

A O Anokhin, V Yu Irkhin and M I Katsnelson
Institute of Metal Physics, 620219 Sverdlovsk, USSR

Received 19 July 1990, in final form 14 November 1990

Abstract. A critical consideration of some approaches to the metal–insulator transition problem, starting from the many-electron representation, is carried out within the framework of the Hubbard and classical s–d models in the far-paramagnetic region. The analytical properties of the corresponding one-electron Green functions are discussed, the importance of terms of sufficiently high orders in $1/z$ being demonstrated. The total energy, electronic specific heat and corrections to the local moment are calculated. The Hubbard-III approximation in the Hubbard model (but not in the s–d model) is shown to lead to difficulties when calculating thermodynamic properties.

1. Introduction

The problem of the Mott transition (metal–insulator transition) driven by the inter-electron correlation [1] is, perhaps, one of the challenges in solid state theory. Recently, this problem has attracted a great deal of attention mainly in connection with the widespread point of view on the high-T_c superconductors, which are considered as narrow-band systems near the Mott transition [2].

Beginning with the pioneering paper by Hubbard [3] (using the method of double-time Green functions) the entire arsenal of many-particle physics methods, such as the functional integral approach [4], the diagram technique [5], the Schwinger formalism [6], the different variational methods [7–9] and the renormalization group method [10] was applied in treating the metal–insulator transition problem. Nevertheless, the physical picture of the transition is still vague. In a large number of papers, starting from [3], the metal–insulator transition is identified with the confluence of the Hubbard subbands and with the disappearance of the Hubbard gap (the band is assumed to be half-filled). In the Hubbard [11] model, such subbands are those of doubly and singly occupied sites, respectively. However, it should be emphasized that the Hubbard model is not the only one to give the metal–insulator transition. As we shall demonstrate further, such a transition is also possible within the s–d exchange model [12]. In real situations, the picture is intermediate between those in the s–d and Hubbard models. For example, in d-metal oxides the Mott transition takes place in one of the crystal-field split subbands (t_{2g} or e_g) on the background of the magnetic moments in another subband [13]; the s–d exchange model is also applied when describing the electron correlations of high-T_c superconductors [14].

0953-8984/91/111475 + 17 $03.50

In the present paper we treat the metal–insulator transition problem in the paramagnetic phase of the Hubbard and s–d exchange models with the aid of the double-time Green function method in the representation of Hubbard many-electron X operators. The use of the s–d model enables one to establish the role of different contributions owing to the formally small parameter $1/2S$, S being spin of the magnetic ions. Special attention is given to the analytical properties of the Green functions obtained and the 'evolution' of the electron spectrum versus the inter-electron interaction parameter and the bare density of electron states. The paper is organized as follows. In section 2 we calculate the one-electron retarded Green functions within the framework of the Hubbard and the classical s–d exchange models. In section 3 the simplest self-consistent equations, and in section 4 the Hubbard-III-type approximation and its analogue in the s–d model, are obtained. In section 5 the consistency of the approximations employed with the $1/z$-perturbation theory is discussed. The results on the metal–insulator transition and the behaviour of some physical quantities (the specific heat and local moment) are presented in section 6 and section 7. In section 8 we present the results of the numerical calculations of the one-electron density of states (DOS) and the optical DOS. The analytical properties of the Green functions obtained are considered in the appendix.

2. Calculation of the one-electron Green function

We treat the problem of the metal–insulator transition within the Hubbard model

$$H = \sum_{k\sigma} t_k c_{k\sigma}^{\dagger} c_{k\sigma} + U \sum_i n_{i\uparrow} n_{i\downarrow} \tag{1}$$

(t_k is the band energy and U is the Hubbard on-site repulsion) and the s–d exchange model

$$H = \sum_{k\sigma} t_k c_{k\sigma}^{\dagger} c_{k\sigma} - I \sum_{i\alpha\beta} \boldsymbol{S}_i \boldsymbol{\sigma}_{\alpha\beta} c_{i\alpha}^{\dagger} c_{i\beta} \tag{2}$$

(I is the s–d exchange parameter, $\boldsymbol{S}_i$ are the localized-spin operators and $\boldsymbol{\sigma}$ are the Pauli matrices). Both models have similar properties, especially for the classical limit of the s–d model ($S \to \infty$ and $IS \to$ constant) which will be considered below. To take into account the Hubbard splitting of the conduction band (e.g. term effects), it is appropriate to use the Hubbard [15] many-electron representation

$$X_i^{\lambda\mu} = |i\lambda\rangle\langle i\mu| \qquad X_i^{\lambda\mu} X_i^{\nu\kappa} = \delta_{\mu\nu} X_i^{\lambda\kappa} \tag{3}$$

where $|i\lambda\rangle$ is the complete set of the states on a site i. For the model (1), $\lambda = 0, \pm, 2$, $|i0\rangle$ being the empty state, $|i\sigma\rangle$ the singly occupied state with the spin projection σ and $|i2\rangle$ being the doubly occupied state (a double). For the model (2), $\lambda = M, \{\mu, \alpha\}, \{\mu, \beta\}, \{M, 2\}, |iM0\rangle$ being the empty state with the localized spin projection M, $|i\mu, \alpha(\beta)\rangle$ the singly occupied state with the total on-site spin moment $S \pm \frac{1}{2}$ and its projection μ, and

$|iM2\rangle$ the doubly occupied state. The interaction Hamiltonian takes the diagonal form in the representation (3)

$$H_{\text{int}} = U \sum_i X_i^{22} \tag{4}$$

$$H_{\text{int}} = -IS \sum_{\mu=-S-\frac{1}{2}}^{S+\frac{1}{2}} X_i^{\mu\alpha,\mu\alpha} + I(S+1) \sum_{\mu=-S+\frac{1}{2}}^{S-\frac{1}{2}} X_i^{\mu\beta,\mu\beta}. \tag{5}$$

The one-electron operators $c_{i\sigma}^\dagger$ are expressed in terms of many-electron X operators by

$$c_{i\sigma}^\dagger = \sum_{\gamma\delta} \langle i\gamma| c_{i\sigma}^\dagger |i\delta\rangle X_i^{\gamma\delta}. \tag{6}$$

For the Hubbard model

$$c_{i\sigma}^\dagger = X_i^{\sigma 0} + \sigma X_i^{2-\sigma} \tag{7}$$

and for the s–d model

$$c_{i\sigma}^\dagger = f_{i\sigma}^\dagger + g_{i\sigma}^\dagger \tag{8}$$

$$f_{i\sigma}^\dagger = \sum_{M=-S}^{S} \left[\left(\frac{S+\sigma M+1}{2S+1} \right)^{1/2} X_i^{M+\sigma/2,\alpha;M} + \left(\frac{S+\sigma M}{2S+1} \right)^{1/2} X_i^{M,2;M-\sigma/2,\beta} \right] \tag{9}$$

$$g_{i\sigma}^\dagger = \sigma \sum_{M=-S}^{S} \left[\left(\frac{S-\sigma M}{2S+1} \right)^{1/2} X_i^{M+\sigma/2,\beta;M} + \left(\frac{S-\sigma M+1}{2S+1} \right)^{1/2} X_i^{M,2;M-\sigma/2,\alpha} \right]. \tag{10}$$

The components of the total on-site spin operator are given by

$$S_{it}^z = \sum_{M=-S}^{S} M(X_i^{M;M} + X_i^{M,2;M,2}) + \sum_{M=-S-\frac{1}{2}}^{S+\frac{1}{2}} M X_i^{M,\alpha;M,\alpha} + \sum_{M=-S+\frac{1}{2}}^{S-\frac{1}{2}} M X_i^{M,\beta;M,\beta} \tag{11}$$

$$\begin{aligned} S_{it}^{-\sigma} = & \sum_{M=-S}^{S} [(S+\sigma M+1)(S-\sigma M)]^{1/2} (X_i^{M;M+\sigma} + X_i^{M,2;M+\sigma,2}) \\ & + \sum_{M=-S-\frac{1}{2}}^{S+\frac{1}{2}} [(S+\tfrac{1}{2}+\sigma M+1)(S+\tfrac{1}{2}-\sigma M)]^{1/2} X_i^{M,\alpha;M+\sigma,\alpha} \\ & + \sum_{M=-S+\frac{1}{2}}^{S-\frac{1}{2}} [(S-\tfrac{1}{2}+\sigma M+1)(S-\tfrac{1}{2}-\sigma M)]^{1/2} X_i^{M,\beta;M+\sigma,\beta}. \end{aligned} \tag{12}$$

In the classical limit, for the paramagnetic state

$$\langle\{f_{k\sigma}, f_{k\sigma}^\dagger\}\rangle = \langle\{g_{k\sigma}, g_{k\sigma}^\dagger\}\rangle = \tfrac{1}{2} \tag{13}$$

and the transitions $0 \to \alpha$, $\beta \to 0$, $2 \to \alpha$, $\beta \to 2$ correspond to the same energy $-IS = -J/2$ so that the Hamiltonian (2) takes a form similar to that of (1), and we have

$$[f_{k\sigma}, H_{\text{int}}] = -(J/2) f_{k\sigma} \qquad [g_{k\sigma}, H_{\text{int}}] = (J/2) g_{k\sigma}. \tag{14}$$

Consider the calculation of the one-electron anticommutator retarded Green function

$$G_{k\sigma}(E) = \langle\langle c_{k\sigma} | c_{k\sigma}^\dagger \rangle\rangle_E = \langle\langle f_{k\sigma} | c_{k\sigma}^\dagger \rangle\rangle_E + \langle\langle g_{k\sigma} | c_{k\sigma}^\dagger \rangle\rangle_E \tag{15}$$

in the classical s–d model ($S \to \infty$, J = constant). From the equations of motion for the Green functions in the right-hand side of (15) one gets

$$\langle\langle f_{k\sigma} | c_{k\sigma}^\dagger \rangle\rangle_E = \frac{\frac{1}{2}}{E+J/2} (1 + t_k \langle\langle c_{k\sigma} | c_{k\sigma}^\dagger \rangle\rangle_E) + \frac{1}{E+J/2} \sum_{q\sigma'} t_q \langle\langle \delta\{f_{k\sigma}, f_{q\sigma'}^\dagger\} c_{q\sigma'} | c_{k\sigma}^\dagger \rangle\rangle_E \tag{16}$$

$$\langle\langle g_{k\sigma}|c^{\dagger}_{k\sigma}\rangle\rangle_E = \frac{\frac{1}{2}}{E - J/2}(1 + t_k\langle\langle c_{k\sigma}|c^{\dagger}_{k\sigma}\rangle\rangle_E) + \frac{1}{E - J/2}\sum_{q\sigma'} t_q\langle\langle \delta\{g_{k\sigma}, g^{\dagger}_{q\sigma'}\}c_{q\sigma'}|c^{\dagger}_{k\sigma}\rangle\rangle_E \tag{17}$$

where $\delta A = A - \langle A\rangle$. Summing equations (16) and (17) we obtain

$$G_{k\sigma}(E) = \frac{E}{E^2 - Et_k - J^2/4} - \frac{J}{E^2 - Et_k - J^2/4}L^{\sigma}_k(E)$$

$$= \sum_{i=1,2}\left[\frac{1}{2} + (-1)^i\left(\frac{t_k}{\varepsilon_k} - \frac{J}{\varepsilon_k}\right)L^{\sigma}_k(E)\right]\frac{1}{E - E_{ki}} \tag{18}$$

where

$$E_{ki} = \tfrac{1}{2}[t_k - (-1)\varepsilon_k] \qquad \varepsilon_k = (t_k^2 + J^2)^{1/2} \tag{19}$$

are the Hubbard-I one-electron energies,

$$L^{\sigma}_k(E) = \tfrac{1}{2}\sum_{q\sigma'} t_q\langle\langle(\delta\{f_{k\sigma}, f^{\dagger}_{q\sigma'}\} - \delta\{g_{k\sigma}, g^{\dagger}_{q\sigma'}\})c_{q\sigma'}|c^{\dagger}_{k\sigma}\rangle\rangle_E$$

$$= \frac{1}{2S}\sum_q t_{k-q}\langle\langle\sigma S^z_q c_{k-q\sigma} + S^{-\sigma}_q c_{k-q,-\sigma}|c^{\dagger}_{k\sigma}\rangle\rangle_E \tag{20}$$

with S^{α}_q being the Fourier components of spin-density operators. Here we have used the anticommutation relations

$$\{f_{k\sigma}, f^{\dagger}_{k-q\sigma}\} - \{g^{\dagger}_{k\sigma}, g_{k-q\sigma}\} = \frac{2\sigma S^z_{qt}}{2S+1} + \frac{1}{2S+1}\sum_{M=-S}^{S}(X^{M,0;M,0}_q - X^{M,2;M,2}_q)$$

$$= \frac{2\sigma S^z_q}{2S+1} + O\left(\frac{1}{2S}\right) \tag{21}$$

$$\{f_{k\sigma}, f^{\dagger}_{k-q,-\sigma}\} = -\{g_{k\sigma}, g^{\dagger}_{k-q,-\sigma}\} = S^{-\sigma}_{qt}/(2S+1). \tag{22}$$

An analogous calculation of the Green functions entering $L^{\sigma}_k(E)$ yields

$$L^{\sigma}_k(E) = -\frac{J}{(2S)^2}\sum_q\frac{t_{k-q}}{\varepsilon_{k-q}}\left(\chi_q + \sum_p t_{k-q+p}\langle\langle(S^z_q S^z_{-p} + S^{\sigma}_q S^{-\sigma}_{-p})c_{k-q+p\sigma} + \sigma(S^z_q S^{-\sigma}_{-p}\right.$$

$$\left. - S^{-\sigma}_q S^z_{-p})c_{k-q+p,-\sigma}|c^{\dagger}_{k\sigma}\rangle\rangle_E\right)\frac{1}{E^2 - Et_{k-q} - J^2/4}. \tag{23}$$

Equations (18) and (23) are exact in the quasiclassical limit. After the decoupling we get

$$L^{\sigma}_k(E) \simeq \frac{J}{(2S)^2}\sum_{i=1,2}\sum_q\frac{t_{k-q}}{\varepsilon_{k-q}}\chi_q\frac{(-1)^i}{E - E_{ki}}[1 + t_k G_{k\sigma}(E)] \tag{24}$$

where $\chi_q = \langle S_q \cdot S_{-q}\rangle$. The decoupling (24) holds to first order in $1/z$, z being the nearest-neighbour number (see section 5). Substituting (24) into (18) we get

$$G_k(E) = \Phi_k(E)[y(E) - \Phi_k(E)t_k]^{-1} \tag{25}$$

$$\Phi_k(E) = 1 + \left(\frac{J}{E}\right)^2\sum_q\frac{\chi_{k-q}t_q/(2S)^2}{y(E) - t_q} \tag{26}$$

where

$$y(E) = E - J^2/4E \tag{27}$$

is the inverse locator in the Hubbard-I approximation.

A similar consideration for the Hubbard model (compare also [16]) yields the same expressions (25) and (26) with the replacement $S \to \frac{1}{2}$, $J \to U$, if we neglect the terms proportional to Fermi excitation occupation numbers and charge fluctuation correlation functions, which are formally small in $1/2S$.

3. The simplest self-consistent approximation

It is easy to see that equations (25) and (26) yield a gap in the density of states for arbitrarily small J. The most natural way to obtain a self-consistent expression for the Green function, describing the metal–insulator transition, is to replace $t_q \to \Phi_q(E)t_q$ in the denominator of the second term of (26). Then we have

$$\Phi_k(E) = 1 + \left(\frac{J}{E}\right)^2 \sum_q \frac{\chi_{k-q} t_q/(2S)^2}{y(E) - \Phi_q(E)t_q}. \tag{28}$$

Such a replacement is in agreement with the result of the $1/z$-perturbation theory in the classical s–d model up to $1/z^2$ (see section 5).

For $\chi_q = S(S+1)$ (far-paramagnetic region), $\Phi(E)$ is independent of k, and the self-consistent equation for the resolvent function

$$R(E) = \sum_k G_k(E) \tag{29}$$

determining the density of states DOS

$$N(E) = -(1/\pi)\,\mathrm{Im}\,[R(E)] \tag{30}$$

takes the form

$$R(E) = R_0[y(E)/\Phi(E)] \equiv R_0(F(E)) \tag{31}$$

$$\Phi(E) = 1 + [J^2\Psi/E^2\Phi(E)]\{[y(E)/\Phi(E)]R(E) - 1\} \tag{32}$$

$$R_0(E) = \sum_k \frac{1}{E - t_k} \qquad N_0(E) = -\frac{1}{\pi}\,\mathrm{Im}\,[R_0(E)] \tag{33}$$

$N_0(E)$ being the bare DOS, and $\Psi = \chi/(2S)^2$. It should be noted that in the case of the classical s–d model ($\Psi = \frac{1}{4}$) the Green function (25) has no poles in the upper half-plane of complex energy variable. For the Hubbard model ($\Psi = \frac{3}{4}$) the function (25) does not possess all the analytical properties of a retarded Green function; it is not analytic in the upper half-plane (see the appendix). This results in the violation of the sum rule

$$L \equiv \int \mathrm{d}E\, N(E) = 1. \tag{34}$$

A self-consistency equation in the Hubbard model, similar to that considered above, yields the same results as those of the Zaitsev [5] approach. For both the Hubbard and the s–d models the self-consistency procedure violates analytical properties. However, this violation is not so important as that resulting from the non-analyticity of the

'unrenormalized' Green function in the case of the Hubbard model (see section 8). Thus, the use of the classical s–d model enables one to improve partially the description of the metal–insulator transition.

4. The Hubbard-III-type self-consistency equation

Equation (26) corresponds to Hubbard's [3] scattering corrections (see equations (31), (32) of that paper). It should be noted that the 'resonance-broadening correction' [3] vanishes in the classical limit. Thus, the alloy analogy is more natural for the classical s–d model than for the Hubbard model.

To obtain an analogue of the Hubbard-III approximation in the classical s–d model we rewrite equations (25) and (26) as

$$F_k(E) \equiv y(E)/\Phi_k(E) = [y(E) - \lambda_k(E)]/[1 - \lambda_k(E)/E] \tag{35}$$

$$\lambda_k(E) = y(E) - \left(\sum_q \frac{\chi_q/S^2}{y(E) - t_{k-q}}\right)^{-1}. \tag{36}$$

In the far-paramagnetic region, equations (35) and (36) coincide with equations (32) and (33) in [3]. The Hubbard-III-type approximation corresponds to replacing $y(E)$ in (36) by the exact inverse locator $F_k(E)$ (with appropriate quasimomenta) defined by

$$G_k^{-1}(E) = F_k(E) - t_k \tag{37}$$

which yields

$$\lambda_k(E) = F_k(E) - \left(\sum_q \frac{\chi_q}{S^2} G_{k-q}(E)\right)^{-1}. \tag{38}$$

Then for χ_q = constant the Hubbard-III-type expression for the Green function may be represented in the form (26) with

$$\Phi(E) = 1 + [J^2\Psi/E^2\Phi(E)][y(E)R(E)/\Phi(E) - 1]/\{1 - (4\Psi/\Phi(E) - 1) \times [y(E)R(E)/\Phi(E) - 1]\} \tag{39}$$

where $\Psi = \frac{1}{4}$. Equation (39) holds for the Hubbard model (see [3]) if we put $\Psi = \frac{3}{4}$. Equations (25) and (39) may be written as

$$G_k(E) = [E - t_k - \Sigma(E)]^{-1} \tag{40}$$

$$\Sigma(E) = (J^2/16\Psi)R(E)/\{1 + \Sigma(E)R(E) + [(4\Psi)^{-1} - 1]ER(E)\}. \tag{41}$$

For the classical s–d model ($\Psi = \frac{1}{4}$) the last term in the denominator of (41) vanishes, and equation (41) is exactly the CPA result for a binary alloy with equal concentrations of components which correspond to the states α and β. For the Hubbard model the situation is more complicated owing to the quantum 'resonance-broadening' corrections [3]. Note that approaches using the static approximation within path integral formalism in the Hubbard model yield CPA-type self-consistency equations and usually neglect the resonance broadening corrections, i.e. are essentially quasiclassical. Unlike the

approximation in the previous section, the Hubbard-III approximation satisfies necessary analytic properties (see, e.g., [17]).

5. Comparison with the $1/z$-perturbation theory

Now we discuss the approximations (32) and (39) from the viewpoint of the $1/z$-perturbation theory. Hereafter we consider the far paramagnetic case. Proceeding as in section 2, the sequence of equations of motion for the one-electron Green function in the classical s–d model is obtained in the form

$$[y(E) - t_k]G_k(E) = 1 - \frac{J}{2SE}\sum_{q_1} t_{k-q_1}\Gamma_{kq_1}(E)$$

$$[y(E) - t_{k-q_1}]\Gamma_{kq_1}(E) = -\frac{J}{2SE}\left(K_{q_1} + \sum_{q_2} t_{k-q_1-q_2}\Gamma_{kq_1q_2}(E)\right)$$

$$\vdots \tag{42}$$

$$[y(E) - t_{k-q_1-\ldots-q_n}]\Gamma_{kq_1\ldots q_n}(E) = \delta_{q_1\ldots+q_n}K_{q_1\ldots q_{n-1}} - \frac{J}{2SE}\left(K_{q_1\ldots q_n} + \sum_{q_1\ldots q_{n+1}} t_{k-q_1-\ldots-q_{n+1}}\Gamma^{\sigma}_{kq_1\ldots q_{n+1}}(E)\right)$$

where we use the notation

$$\Gamma^{\sigma}_{kq_1\ldots q_n}(E) = \langle\langle S^{\dagger}_{q_1\sigma}\hat{S}_{q_2\sigma}\ldots\hat{S}_{q_n\sigma}c_{k-q_1-\ldots q_n,\sigma}|c^{\dagger}_{k\sigma}\rangle\rangle_E \tag{43}$$

$$K_{q_1\ldots q_n} = \langle S^{\dagger}_{q_1\sigma}\hat{S}_{q_2\sigma}\ldots\hat{S}_{q_n\sigma}S_{q_1+\ldots q_n\sigma}\rangle \tag{44}$$

$$S^{\dagger}_{q\sigma} = (\sigma S^z_q, S^{-\sigma}_q) \qquad \hat{S}_{q\sigma} = \begin{pmatrix}\sigma S^z_q & S^{-\sigma}_q\\ S^{\sigma}_q & -\sigma S^z_q\end{pmatrix} \qquad c_{k\sigma} = \begin{pmatrix}c_{k,\sigma}\\ c_{k,-\sigma}\end{pmatrix}. \tag{45}$$

It follows from (31), (32) and (42) that the Green function may be represented as

$$G_k(E) = \Phi_k(E)/[y(E) - t_k\Phi_k(E)] \tag{46}$$

where

$$\Phi_k(E) = 1 + \{\Pi_k(E)\}_{\text{irr}} \tag{47}$$

$$\Pi_k(E) = \sum_{n=1}^{\infty}\left(\frac{J}{2SE}\right)^{2n}\sum_{q_1\ldots q_{2n-1}} Q_{k-q_1}\ldots Q_{k-q_1-\ldots-q_{2n-1}}K_{q_1\ldots q_{2n-1}} \tag{48}$$

$$Q_q(E) = t_q/[y(E) - t_q] \tag{49}$$

where the subscript irr means that the contributions which diverge at $y(E) = t_k$ must be omitted. In the classical limit $S \to \infty$, the spin correlation function may be decoupled to obtain

$$K_{q_1} = \chi = S(S+1) \tag{50}$$

$$K_{q_1q_2q_3} = \chi^2(\delta_{q_1+q_2} + \delta_{q_2+q_3} - \tfrac{1}{3}\delta_{q_1+q_3}) - \tfrac{2}{3}\chi^2. \tag{51}$$

Consider the expansion of (47) in the series with respect to $1/z$, nth order corresponding to n summations over quasimomenta

$$\Phi_k(E) = 1 + \sum_{n=1}^{\infty} \Phi_k^{(n)}(E). \tag{52}$$

To second order in $1/z$, one obtains

$$\Phi_k^{(1)}(E) = \left(\frac{J}{2SE}\right)^2 \chi \sum_p Q_p \tag{53}$$

$$\Phi_k^{(2)}(E) = \left(\frac{J}{2SE}\right)^4 \chi^2 \sum_{qp} Q_q^2 Q_p - \frac{1}{3}\left(\frac{J}{2SE}\right)^4 \chi^2 \sum_{qp} Q_{k-q} Q_{q-p} Q_p. \tag{54}$$

Retaining only the first-order contribution in (52) we obtain the approximation (26). Noting that the first term in (54) gives the renormalization of the denominator in (26) up to the first order in $1/z$ and considering the higher orders in the expansion (47) we may extract the infinite sequence corresponding to the approximation (32). In the third order, there arises the term

$$\delta\Phi^{(3)}(E) = -\tfrac{2}{3} \sum_{qpr} Q_q Q_p Q_r \left(\frac{J}{2E}\right)^4 \tag{55}$$

which comes from the last term in (51) (all spins on one site), and also a large number of 'connected' terms. The term (55) differs from the third-order term arising from the expansion of the Hubbard-III approximation by a factor of $\frac{2}{3}$. (Note that for the corresponding SU(N) model this factor reads $N/(N+1)$, so that the discrepancy vanishes in the large-N limit.) Picking out from the second term in (54) the contribution on a site (i.e. averaging over k) we may restore the agreement. Carrying out the same trick in all corresponding higher-order terms of the perturbation series we obtain

$$\Phi(E) = 1 + \left(\frac{J}{2E}\right)^2 \sum_q Q_q \left[1 + \left(\frac{J}{2E}\right)^2 \sum_{rp} Q_r Q_p\right]^{-1}. \tag{56}$$

Replacing

$$Q_q(E) \to \tilde{Q}_q(E) = t_q/[y(E) - \Phi(E) t_q] \tag{57}$$

and using the transformation

$$\left(\frac{J}{2E}\right)^2 \sum_q \tilde{Q}_q(E) = \Phi(E) - 1 + O\left(\frac{1}{z^2}\right) \tag{58}$$

we rederive equation (39) with $\Psi = \frac{1}{4}$. Thus, from the viewpoint of the $1/z$-perturbation theory in the classical s–d model, the Hubbard-III self-consistent approximation differs

from the simplest one by terms of sufficiently high order, so that the latter are rather important for fulfilling analytical properties.

6. The metal–insulator transition

As follows from (25) and (31) the density of states on the Fermi level ($E = 0$) does not vanish if the asymptotical behaviour of $\Phi(E)$ coincides with that of $y(E)$, i.e. the quantity

$$\alpha(J) = \lim_{E\to 0} [y(E)/\Phi(E)] \tag{59}$$

is finite. Then we obtain the equation for $\alpha(J)$

$$J^2/4 = 4\Psi\alpha^2[\alpha R_0(\alpha) - 1] \tag{60}$$

in the approximation (32), and

$$J^2/4 = 4\Psi\alpha[\alpha - R_0^{-1}(\alpha)] \tag{61}$$

in the Hubbard-III approximation. Near the metal–insulator transition, α is large in the absolute value (real in the insulator phase and imaginary in the metallic phase) and is divergent at the transition point, so that we may use the expansion

$$R_0(\alpha) = 1/\alpha + \mu_2/\alpha^3 + \mu_4/\alpha^5 + \dots \tag{62}$$

where μ_n are the moments of the bare DOS which is assumed to be symmetric. Then we obtain from both (60) and (61) the critical value of J

$$|J_c| = 4\sqrt{\Psi\mu_2} \tag{63}$$

$$\alpha(J \to J_c) \simeq (2M/J_c(J - J_c))^{1/2} \tag{64}$$

where $M = \mu_4$ and $M = \mu_4 - \mu_2^2$ for the approximations (32) and (39), respectively. For the semielliptic conduction band, equations (60) and (61) may be solved exactly, which yields the results of [3, 5]. Using the expansion

$$F(E) = y(E)/\Phi(E) = \alpha(J) + \beta(J)E + \dots \tag{65}$$

we obtain

$$\beta(J) = -\alpha^4(J)/8\Psi M. \tag{66}$$

For the insulator phase the expansion is valid if E lies in the energy gap (outside the gap,

we must use the expansion in inverse powers of E). Thus the width of the gap Δ is estimated from the condition $|\alpha| \sim |\beta|\Delta$ which yields

$$\Delta \propto \Psi |J_c|^{2/3} (2M)^{-1/2} |J - J_c|^{3/2} \theta(|J| - |J_c|). \tag{67}$$

Using the expansion (65), one sets the scaling behaviour for the function $F(E, J)$ near the point of the Mott transition ($J \to J_c$, $\alpha \to \infty$):

$$F(E, J) = \alpha(J) f(E/\Delta(J)) \equiv \alpha(J) f(E\alpha^3(J)). \tag{68}$$

7. Total energy, local moments and thermodynamic properties

Averaging the Hamiltonian we derive for the s–d model

$$\langle H \rangle = \langle H_{\text{kin}} \rangle - 2I\langle S \cdot s \rangle \qquad s_i = \tfrac{1}{2} \sum_{\alpha\beta} c_{i\alpha}^{\dagger} \sigma_{\alpha\beta} c_{i\beta}. \tag{69}$$

Using the equation of motion for the one-electron Green function and the spectral representation yields

$$2 \int \mathrm{d}E \, E f(E) N(E) - \langle H_{\text{kin}} \rangle = -2I\langle Ss \rangle$$

$$\langle H \rangle = 2 \int \mathrm{d}E \, E f(E) N(E) \tag{70}$$

where the factor of 2 comes from the summation over spin projection. At the same time, for the Hubbard model, where the local moments and current carriers belong to the same electron system, we have

$$\int \mathrm{d}E \, E f(E) N(E) - \langle H_{\text{kin}} \rangle = 2UN_2$$

$$\langle H \rangle = \frac{1}{2} \left(-\frac{1}{\pi} \right) \sum_{k\sigma} \int \mathrm{d}E \, (E + t_k) f(E) \, \mathrm{Im} G_{k\sigma}(E) \tag{71}$$

with $N_2 = \langle n_{i\uparrow} n_{i\downarrow} \rangle$ the number of doubles. Near the metal–insulator transition, substituting (68), (30) and (31) into (70) and (71) gives the singular contribution to $\langle H \rangle$ at $T = 0$:

$$\delta\langle H \rangle \propto |\alpha(J)|^{-7} \propto |J - J_c|^{7/2} \theta(|J_c| - |J|) \tag{72}$$

which corresponds to the $3\frac{1}{2}$-order transition (cf [5]). We see that large one-electron damping leads to the weakening of the singularity in the total energy. (In the absence of the one-electron damping and for the square root behaviour of the DOS near the gap, $N(E) \propto \sqrt{E}$; the transition is of $2\frac{1}{2}$ order.) For the square of the total spin on a site we have

$$\langle S_{\text{tot}}^2 \rangle = S(S + 1) - 2\nu S + \mathrm{O}(1)$$

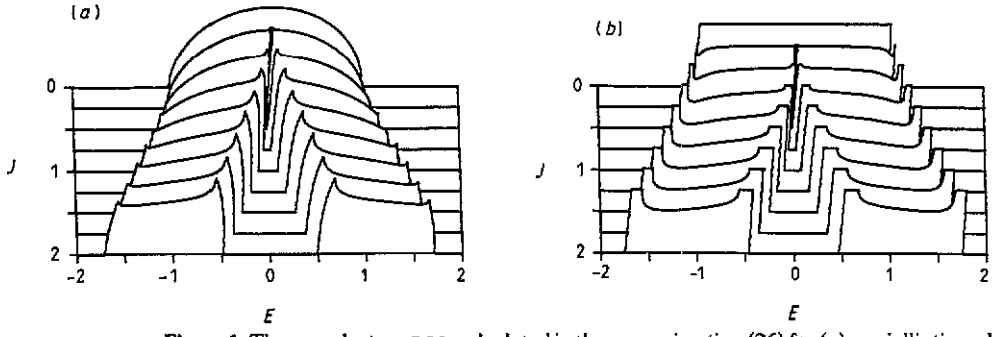

Figure 1. The one-electron DOSS calculated in the approximation (26) for (*a*) semielliptic and (*b*) rectangular bare DOSS.

where $\nu = -\langle Ss\rangle/S$ (for the Hubbard model, $\langle S^2\rangle = \frac{3}{4}(1 - 2N_2)$). The spectral representation gives

$$\nu = -\frac{1}{\pi J}\sum_{k\sigma}\int \mathrm{d}E\,(E - t_k)f(E)\,\mathrm{Im}G_{k\sigma}(E) \tag{73}$$

and for $J \to \pm\infty$ we obtain

$$\nu = [-\tfrac{1}{2} + \mathrm{O}(1/J^2)]\,\mathrm{sgn}\,J \tag{74}$$

so that in the extremely narrow-band limit the total spin on a site equals $S \pm \frac{1}{2}$.

Now we calculate the electronic specific heat $C(T)$. For the s–d model we obtain from (70)

$$C(T) = \partial\langle H\rangle/\partial T = (\pi^2/3)2N(E_\mathrm{F})T. \tag{75}$$

Formally, this expression has a Fermi-liquid-theory form. However, $N(E)$ itself is determined by non-quasiparticle states (the one-electron damping is very large). On the other hand, for the Hubbard model, equation (71) gives

$$C(T) = (\pi^2/3)\{N(E_\mathrm{F}) - (1/\pi)(\partial/\partial E)\,\mathrm{Im}[F(E)R(E)]|_{E=E_\mathrm{F}}\}T. \tag{76}$$

Near the transition ($U \to U_c$), the second term in the curly brackets dominates and we obtain from (76)

$$C(T) \simeq -(\pi^2/3)(\mu_2/3\pi M)\,\mathrm{Im}[\alpha(U)]\,T < 0. \tag{77}$$

Using the Hellman–Feynman theorem

$$N_2 = \partial\mathcal{F}(U)/\partial U$$

and restoring the free energy $\mathcal{F}$ we obtain at $U \to U_c$

$$C(T) = -T\,\partial^2\mathcal{F}/\partial T^2 = \tfrac{1}{6}(\pi^2/3)2N(E_\mathrm{F})T \tag{78}$$

(where we used equations (63), (64) and (66)), so that the calculated $C(T)$ is smaller than that of non-interacting electrons with the DOS $N(E)$. This result is rather unusual and drastically different from that for Fermi-liquid systems where correlation effects lead to $C(T)$ enhancement.

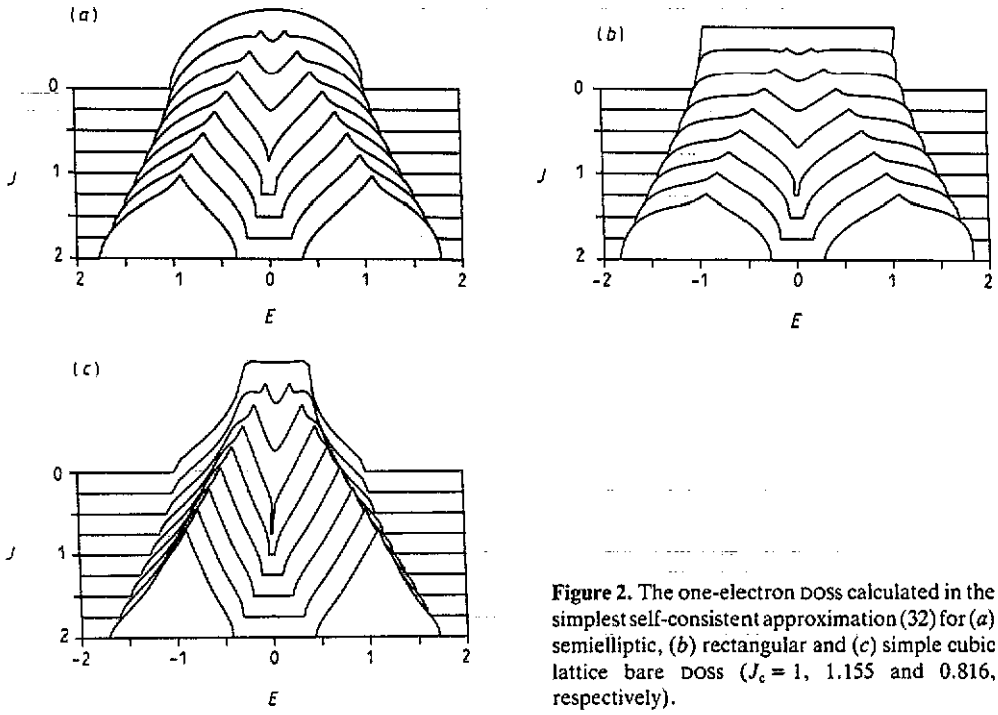

Figure 2. The one-electron DOSS calculated in the simplest self-consistent approximation (32) for (*a*) semielliptic, (*b*) rectangular and (*c*) simple cubic lattice bare DOSS ($J_c = 1$, 1.155 and 0.816, respectively).

Thus, the approximations employed are not quite satisfactory for calculating the specific heat in the Hubbard model. At the same time, for the classical s–d model the use of the Hellman–Feynman theorem, $\nu = \partial\mathcal{F}/\partial J$, gives the same result for $C(T)$ as (75).

8. Results of numerical calculations

The DOSS $N(E)$, calculated in the classical s–d model for the non-self-consistent approximation (26), the simplest self-consistent approximation (32) and the Hubbard-III approximation are shown in figures 1–3 versus J for some bare DOSS (the results in the Hubbard model are qualitatively similar). Despite the violation of analytical properties (leading to occurrence of 'false' singularities at $E = \pm J/2$), the results for the approximation (32) are on the whole similar to those for the more complicated Hubbard-III approximation. The violation of the normalization condition (34) is numerically small at not too large J. On the other hand, for the Hubbard model, where analytical properties are violated even before carrying out the self-consistency procedure, the violation is strong (table 1).

Besides the presence of the energy gap at small J (which is, however, very small), an important drawback of the non-self-consistent approximation is the occurrence of the non-physical DOS peaks near the band edges, which are smeared for more advanced approximations. It should be noted that the form of $N(E)$ for the self-consistent approximations is weakly dependent on the bare DOS form at not too small J (in particular, the Van Hove singularities for the simple cubic lattice are smeared). This is due to a large electron damping.

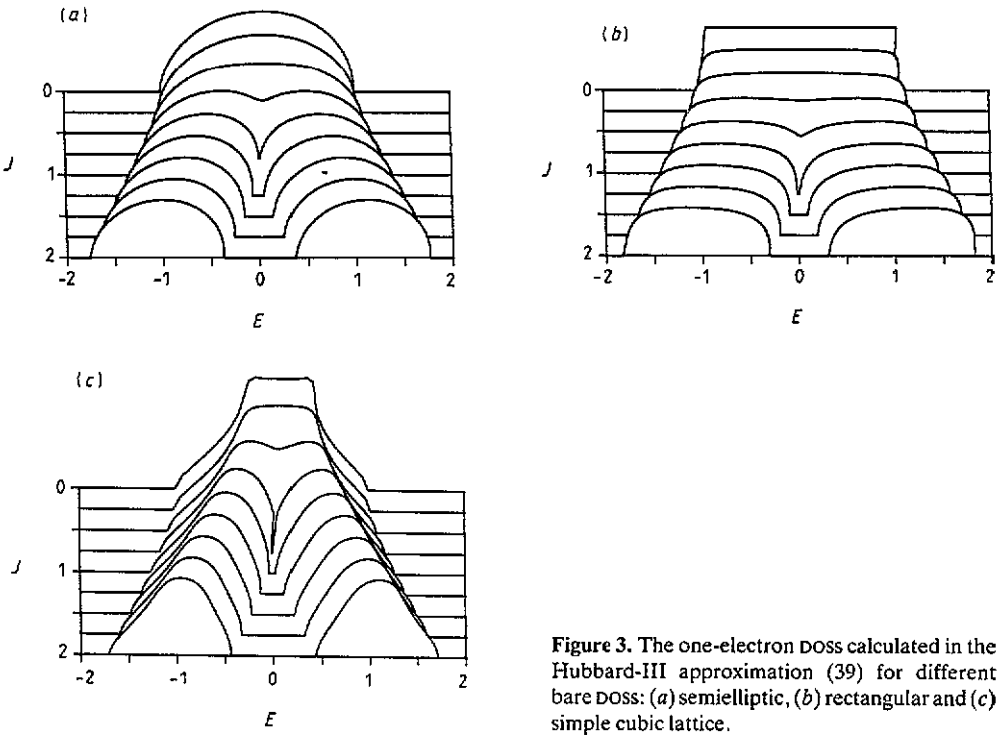

Figure 3. The one-electron DOSS calculated in the Hubbard-III approximation (39) for different bare DOSS: (*a*) semielliptic, (*b*) rectangular and (*c*) simple cubic lattice.

Table 1. The values of the normalization factor L (34) for different approximations and bare DOS: I, approximation (26) for the Hubbard model; II, self-consistent approximation (32) for the Hubbard model; III, self-consistent approximation (32) for the quasiclassical s–d model.

	Normalization factor L								
	Semielliptic bare DOS			Rectangular bare DOS			Simple cubic lattice		
J	I	II	III	I	II	III	I	II	III
0.00	1.00	1.00	1.00	1.00	1.00	1.00	1.00	1.00	1.00
0.25	0.91	0.97	0.98	0.92	0.96	0.99	0.90	0.98	0.98
0.50	0.97	1.02	1.00	0.92	0.97	0.99	1.06	1.09	1.02
0.75	1.11	1.11	1.03	1.02	1.05	1.01	1.21	1.17	1.04
1.00	1.22	1.19	1.05	1.14	1.12	1.02	1.31	1.27	1.06
1.25	1.29	1.26	1.06	1.22	1.19	1.04	1.37	1.31	1.07
1.50	1.38	1.27	1.07	1.27	1.24	1.05	1.40	1.34	1.07
1.75	1.38	1.30	1.07	1.33	1.26	1.06	1.43	1.35	1.08
2.00	1.40	1.33	1.07	1.34	1.28	1.06	1.44	1.35	1.08

The optical DOS

$$\rho(\omega) = \int_{E_F-\omega}^{E_F} \mathrm{d}E\, N(E)N(E+\omega) \tag{79}$$

which defines the indirect optical absorption is shown in figure 4. One can see the

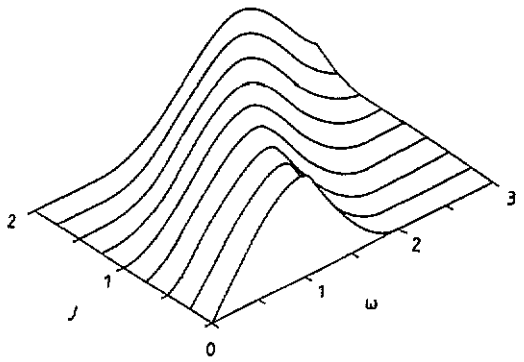

Figure 4. The optical DOS (79) calculated in the Hubbard-III approximation for the semielliptic bare DOS.

Table 2. Correlation energy E_{corr} (80) for the Hubbard model in units of the half of the bare band width, calculated within different approximations and for different bare DOSs: I, Hubbard-I approximation; II, the approximation (26); III the simplest self-consistent approximation (32); (IV), Hubbard-III approximation for the semielliptic, rectangular and simple cubic lattice bare DOSs ($E_{kin}(J=0) = -0.42$, -0.50 and -0.33, respectively).

	E_{corr}			
J	I	II	III	IV
		Semielliptic bare DOS		
0.25	0.02	0.04	0.03	−0.004
0.50	0.02	0.08	0.04	−0.04
1.00	−0.01	−0.01	−0.04	−0.16
1.50	−0.09	−0.16	−0.16	−0.35
2.00	−0.18	−0.34	−0.30	−0.58
		Rectangular bare DOS		
0.25	0.03	0.04	0.03	−0.004
0.50	0.03	0.10	0.06	−0.002
1.00	0.01	0.04	−0.01	−0.06
1.50	−0.05	−0.09	−0.11	−0.30
2.00	−0.14	−0.24	−0.24	−0.46
		Simple cubic lattice		
0.25	0.02	0.05	0.03	−0.002
0.50	0.01	0.04	0.01	−0.01
1.00	−0.04	−0.08	−0.09	−0.04
1.50	−0.13	−0.25	−0.23	−0.09
2.00	−0.24	−0.43	−0.38	−0.21

broad maximum at $\omega \sim J$ corresponding to transitions between the Hubbard subbands. Possibly, such transitions were observed in optical spectra of strongly correlated metals CrO_2 and MoO_2 [18] and of many Mott [1] insulators.

Calculated for various approximation values of the correlation energy

$$E_{corr} = \langle H \rangle - E_{kin}(J=0) \tag{80}$$

(for the Hubbard model, the energy E is referred to the chemical potential $\mu = U/2$) are

Table 3. The same data as table 2 but for the classical s–d model.

	E_{corr}			
J	I	II	III	IV
		Semielliptic bare DOS		
0.25	−0.02	−0.01	−0.01	−0.01
0.50	−0.07	−0.05	−0.06	−0.05
1.00	−0.23	−0.21	−0.24	−0.20
1.50	−0.44	−0.41	−0.47	−0.41
2.00	−0.65	−0.64	−0.72	−0.64
		Rectangular bare DOS		
0.25	−0.02	−0.01	−0.01	−0.01
0.50	−0.05	−0.04	−0.04	−0.04
1.00	−0.20	−0.18	−0.20	−0.17
1.50	−0.40	−0.36	−0.41	−0.36
2.00	−0.62	−0.59	−0.65	−0.58
		Simple cubic lattice		
0.25	−0.02	−0.02	−0.02	−0.000
0.50	−0.09	−0.07	−0.08	−0.002
1.00	−0.28	−0.26	−0.29	−0.04
1.50	−0.50	−0.47	−0.53	−0.12
2.00	−0.73	−0.70	−0.79	−0.23

listed in tables 2 and 3. One can see that, in the case of the Hubbard model, all the approximations under consideration (except the Hubbard-III approximation) yield a non-monotonic correlation energy behaviour with $\langle H \rangle > E_{HF}$ for $U < 1$. On the other hand, for the s–d model, E_{corr} is negative and monotonic at all J.

9. Conclusions

Our consideration demonstrates that some simple Green function approaches using the many-electron representation and describing the metal–insulator transition are not quite satisfactory. In particular, approximations, which are simpler than that of Hubbard [3], violate the analytical properties of Green functions. The drawbacks may be partially removed by passing to the classical s–d model. From the viewpoint of the $1/z$-perturbation theory, the Hubbard-III approximation corresponds to the summation of some sequence, where not even all second-order terms are treated accurately.

The structure of the DOS within the self-consistent approximations under consideration turns out to be rather poor; the detailed structure of the bare DOS is smeared, and no new non-trivial physical features occur. Apparently, the latter is due to neglecting contributions which depend on Fermi excitation distribution functions and violate the rigid-band picture, thereby leading to a strong E-dependence of DOS (e.g. Kondo-like effects [19]). Such effects have a quantum nature and correspond to terms formally small in $1/2S$. Another factor important for the DOS structure is the short-range antiferromagnetic order and spin dynamics which may be included by consideration of the

q- and ω-dependences of the spin correlation function $\chi_{q\omega}$. The treatment of these problems seems to be of great interest for the theory of strongly correlated systems.

Appendix. Analytical properties of the Green functions

Let us verify the analyticity in the upper half-plane of the Green functions used (this requirement is necessary for retarded Green functions). For the non-self-consistent version of (26) we consider

$$\Phi(E) = 1 + (J^2\Psi/E^2)[y(E)R_0(y(E)) - 1] \tag{A1}$$

(for simplicity, we discuss the case χ = constant). For the Hubbard model ($J = U$, $\Psi = \frac{3}{4}$) we have for arbitrary $0 < \delta \ll U/2$

$$\Phi(U/2 + i\delta) = -2[1 - 3\delta\pi N_0(0)] + O(\delta/U)$$

and we get

$$\mathrm{Im}[R(U/2 + i\delta)] = \mathrm{Im}\{R_0[2i\delta/\Phi(U/2 + i\delta)]\} > 0$$

for $\delta < [3\pi N_0(0)]^{-1}$. Thus the DOS is not positively defined and the function $R(E) = \Sigma_k G_k(E)$ is not analytic in the upper half-plane. On the other hand, for the classical s–d model ($J = 2IS$, $\Psi = \frac{1}{4}$)

$$\mathrm{Im}[R(E)] = \mathrm{Im}\{R_0[y(E)/\Phi(E)]\}$$

is negative at $\mathrm{Im}\, E > 0$ since

$$\mathrm{Im}[y(E)/\Phi(E)] = \mathrm{Im}\{E[1 + (J^2/4E)R_0(y(E))]^{-1}\} > 0.$$

For the self-consistent version, the function $\Phi(E)$ defined by the equation

$$\Phi(E) = 1 + [J^2\Psi/E^2\Phi(E)]\{[y(E)/\Phi(E)]R(E) - 1\} \tag{A2}$$

has the branch cut along the imaginary axis in the upper half-plane. To demonstrate this we calculate the quantity

$$A = \lim_{\delta \to 0} \{\mathrm{Im}[\Phi(\pm J/2 + \delta) - \Phi(\pm J/2 - \delta)]\}.$$

Putting $E = \pm (J/2 \pm \delta) + i0$ in (A2), we obtain two solutions:

$$\Phi_1 \equiv \Phi(\pm J/2 + 0) = \tfrac{1}{2}(1 - i\sqrt{16\Psi - 1})$$

$$\Phi_2 \equiv \Phi(\pm J/2 - 0) = \tfrac{1}{2}(1 + i\sqrt{16\Psi - 1})$$

where we have used the fact that $\mathrm{Im}\, \Phi$ changes its sign when crossing the lines $\mathrm{Re}\, E = \pm J/2$. Thus $A = -\sqrt{16\Psi - 1}$ and the Green function (32) is non-analytic (has a branch cut) in the upper half-plane for both the Hubbard and the s–d models. The Hubbard-III approximation (39), which corresponds to the CPA approximation, satisfies the necessary analytical properties. In particular, it follows from (39) that $\Phi(\pm J/2) = 0$.

References

[1] Mott N F 1974 *Metal–Insulator Transitions* (London: Taylor and Francis)

[2] Anderson P W 1987 *Science* **235** 1186; 1988 *Proc. Int. School of Physics 'Enrico Fermi' (Varenna)* (Amsterdam: North-Holland)
[3] Hubbard J 1964 *Proc. R. Soc.* A **281** 401
[4] Cyrot M 1970 *Phys. Rev. Lett.* **25** 871
[5] Zaitsev R O 1978 *Zh. Eksp. Teor. Fiz.* **75** 2362
[6] Arai T and Cohen M H 1980 *Phys. Rev.* B **21** 3300, 3309, 3320
[7] Gutzwiller M C 1965 *Phys. Rev.* **137** A1726
[8] Brinkman W F and Rice T M 1970 *Phys. Rev.* B **2** 4302
[9] Katsnelson M I and Irkhin V Yu 1984 *J. Phys. C: Solid State Phys.* **17** 4291
[10] Hirsh J E 1980 *Phys. Rev.* B **22** 5259
[11] Hubbard J 1963 *Proc. R. Soc.* A **276** 238
[12] Vonsovsky S V 1974 *Magnetism* vol 2 (New York: Wiley)
[13] Terakura K, Oguchi T, Williams A R and Kuebler J 1984 *Phys. Rev.* B **30** 4734
[14] Hatsugai Y, Imade M and Nagaoka N 1989 *J. Phys. Soc. Japan* **58** 1347
[15] Hubbard J 1965 *Proc. R. Soc.* A **285** 542
[16] Irkhin V Yu and Katsnelson M I 1988 *Fiz. Metall. Metalloved.* **66** 41
[17] Ehrenreich H and Schwartz L 1976 *Solid State Physics* vol 31 (New York: Academic)
[18] Chase L L 1974 *Phys. Rev.* B **10** 2226
[19] Irkhin V Yu and Katsnelson M I 1989 *Z. Phys.* B **75** 67